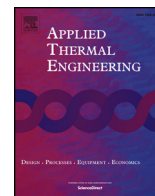




ELSEVIER

Contents lists available at ScienceDirect

Applied Thermal Engineering

journal homepage: www.elsevier.com/locate/apthermeng

Research Paper

Design and performance evaluation of novel personal cooling garment

Jin Hou^a, Zhiwei Yang^b, Peng Xu^{b,*}, Gongsheng Huang^a^a Department of Architecture and Civil Engineering, City University of Hong Kong, Kowloon 999077, Hong Kong^b Department of Mechanical and Energy Engineering, Tongji University, Shanghai 201804, China

HIGHLIGHTS

- A new type of PCG, the PCM-liquid cooling vest (PLV), is developed.
- The PLV is designed and tested using mathematical modeling and human trial.
- The PLV has three operating modes.
- The cooling-storage of the PLV can be finished within 40 min.
- The PLV provides effective cooling for users working indoors for at least two hours.

ARTICLE INFO

Keywords:

Personal cooling garment
Phase change material
Mathematical modeling
Human trial

ABSTRACT

Personal cooling garments (PCGs) have been developed to reduce heat stress and improve human thermal comfort in hot environments. In this study, a new type of PCG, a PCM-liquid cooling vest (PLV), is developed to improve the ease of use of phase change material (PCM) garments. The PLV adopts the scheme of combining PCM with water pipes buried in the PCM. The PCM in the vest is used to cool the torso and the water pipe buried in the PCM circulates cold water from a microchiller to freeze the PCM. This PLV is designed and tested using mathematical modeling and human trial. Based on the simulation results, inorganic PCM with high density and conductivity, a high flow rate of cold water, and multiple parallel water pipes buried in PCM are recommended. Adjusting the tightness and wearing the insulation vest are effective methods to enhance the comfort and prolong the service time of the PLV, respectively. In the human trial, a PLV containing inorganic PCM and with a total mass of 1.8 kg is fabricated and used. The experimental results show that the fabricated PLV can provide effective cooling for at least two hours for users working indoors, without sacrificing the overall thermal comfort in the wearing mode. The cooling-storage can be finished within 40 min in the cooling-storage mode or within 60 min in the cooling-storage and wearing combined mode.

1. Introduction

Working in hot industrial environments [1], wearing impermeable protective clothing [2] or exercising [3] generally increase the heat stress of the human body. Under conditions in which air-conditioning systems are not effective, the use of personal cooling garments (PCGs) is an effective way to reduce heat stress and improve the thermal comfort of the human body by absorbing the excessive heat of a part of the body or the entire body [2,4,5].

Current PCGs are of primarily three types based on the cooling technology: air cooling garments (ACGs), liquid cooling garments (LCGs), and phase change cooling garment (PCCGs) [6]. ACGs distribute ambient or cooled air throughout the garment to enhance sweat evaporation and heat convection between the air and the skin [7]. LCGs

circulate cold liquid inside a garment to eliminate the wearer's heat on the basis of conductive cooling [8]. PCCGs use the latent heat of PCM for cooling the body [9–11]. In addition, other types of PCGs have been designed using water evaporation [12,13], and vacuum desiccant cooling [14], among other techniques. At present, although various PCGs have been reported in the literature and patents, few products satisfy the need of the wearers considering all aspects. ACGs and LCGs are known to provide efficient cooling for prolonged durations; however, the user's movement is restricted owing to the presence of auxiliary cooling devices, such as vapor compression systems and pumps, required for supplying the cooled fluid [15,16]. For example, the overall cooling system designed by Timothy C. for duty personnel has a mass of 5.31 kg [15]. Although PCCGs are more portable than ACGs and LCGs, they have the drawback of having a short period of effectiveness

* Corresponding author.

E-mail address: xupeng@tongji.edu.cn (P. Xu).<https://doi.org/10.1016/j.applthermaleng.2019.02.013>

Received 11 October 2018; Received in revised form 22 January 2019; Accepted 5 February 2019

Available online 07 March 2019

1359-4311/ © 2019 Elsevier Ltd. All rights reserved.

Nomenclature	
<i>Variables</i>	
<i>B</i>	blood perfusion rate, kg/(s·m ³)
<i>c</i>	specific heat, J/kg·°C
<i>f</i>	signal, °C
<i>K</i>	weighting coefficient
<i>Q</i>	heat source, W/m ³
<i>q</i>	heat transfer rate, W/m ²
<i>R</i>	dynamic induction, s
<i>S</i>	surface area, m ²
<i>T</i>	temperature, °C
<i>v</i>	ambient air velocity, m/s
λ	thermal conductivity, W/m·°C
ρ	density, kg/m ³
τ	time, s
<i>Subscripts</i>	
<i>a</i>	ambient air
<i>b</i>	blood
<i>ba</i>	basal state
<i>co</i>	core (hypothalamus)
<i>e</i>	evaporation
<i>es</i>	sweating
<i>i</i>	segment number
<i>m</i>	metabolism
<i>s</i>	skin
<i>set</i>	set point
<i>t</i>	tissue
<i>vc</i>	vasoconstriction
<i>vd</i>	vasodilation
<i>Acronyms</i>	
ACG	air cooling garment
PCCG	phase change cooling garment
PCM	phase change material
PVC	polyvinyl chloride
LCG	liquid cooling garment
PCG	personal cooling garment
PLV	PCM-liquid cooling vest
TPU	thermoplastic polyurethane

[6,17]. PCCGs require cooling-storage in refrigerators or cold water, which interrupts the cooling process for another cooling-storage time and makes the use of PCCGs inconvenient. Thus, more design concepts and research are required in terms of PCGs to make such garments more comfortable and convenient.

In the design and research of PCGs, human trial, manikin testing and mathematical modeling are the three main methods to examine the new concepts, optimize the design parameters, and assess the PCGs' cooling performance [18]. The human trial is the most direct and appropriate way to evaluate a PCGs' cooling effect; however, it is expensive and time-consuming because a sufficient number of test samples is needed. In Guan's research, human trial was used to explore the optimal design of a phase change suit for medical use [19]. Twenty-three volunteers cast thermal comfort votes for several suits with different distribution PCM packets to evaluate the design of the suit. Manikin testing has better repeatability and lower cost compared to human trials [20]. Li-Lina evaluated the cooling performance of three different cooling garments by using movable sweating thermal manikin 'Walter' in a temperature cabin [21]. However, manikins with the thermophysiological function are often unsatisfactory for validation owing to the technical limitation of appropriately controlling manikins using thermophysiological models [22]. For mathematical modeling, models of the human body, PCG, and the environment are built to simulate the thermal interactions between the human body, PCG, and the environment [23]. With the help of computers, mathematical modeling makes it easy to determine the various parameter fields of PCGs and the body, and thereby evaluate the cooling performance of PCGs. In addition, by modifying settings of the PCG model, optimal design parameters can be found easily and rapidly. Therefore, mathematical modeling is a valuable tool for the design and research of PCGs and has been widely used in previous studies [24]. For example, M. Mokhtari Yazdi built models of the torso skin and the PCM cooling vest to simulate heat transfer between the skin and PCM, with the help of ANSYS software [11].

In this paper, we propose a new type of PCG, the PCM-liquid cooling vest (PLV), to improve the convenience of cooling-storage for conventional PCM garments. The vest adopts the scheme of combining PCM with water pipes buried in the PCM. The PCM in the vest is used to cool the torso and the water pipe buried in the PCM is used to circulate cold water from a microchiller to freeze the PCM. Based on this design scheme, when the vest is separated from the microchiller, the PLV provides freedom of movement to the wearer, similar to the traditional

PCM garments. When the PLV is connected to the microchiller to be charged by the circulated cold water, the PLV can be set aside or worn by the wearer to cool his/her body, if needed.

In the development of this new type of PCG, mathematical modeling and human trial are used for the design and performance evaluation of the PLV. The mathematical modeling is used to predict the operating performance of the PLV under different working conditions and to investigate multiple design parameters. A set of trials is conducted to validate the simulation results by the mathematical modeling and evaluate the thermal sensation and comfort of the PLV.

2. PCM-liquid cooling vest

This new type of PCG, as illustrated in Fig. 1, adopts the scheme of combining the PCM with water pipes buried in the PCM. The PCM in the vest is used to cool the torso, which has a high cooling capacity [11,25]. The water pipe buried in the PCM circulates cold water from a microchiller to freeze the PCM. The PLV has three operating modes: cooling-storage mode, wearing mode, and cooling-storage and wearing combined mode. In the cooling-storage mode, the microchiller is connected to the vest and supplies cold water to the vest to freeze the PCM. In the wearing mode, the vest is separated from the microchiller and worn by the wearer to cool the body. In the cooling-storage and wearing combined mode, the vest is worn by the wearer to cool the body and connected to the microchiller to be charged by the circulated cold water. Using this design, the PLV draws on the advantages of the PCCGs corresponding to high portability and avoidance of the interruption of the cooling process for another cooling-storage time.

The detailed structure of the vest is shown in Fig. 2. The PCM in the vest is packaged with a thermoplastic polyurethane (TPU) film into 16

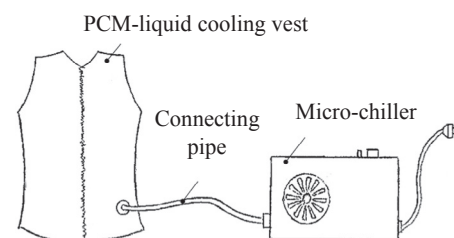


Fig. 1. PCM-liquid cooling vest with the auxiliary microchiller.

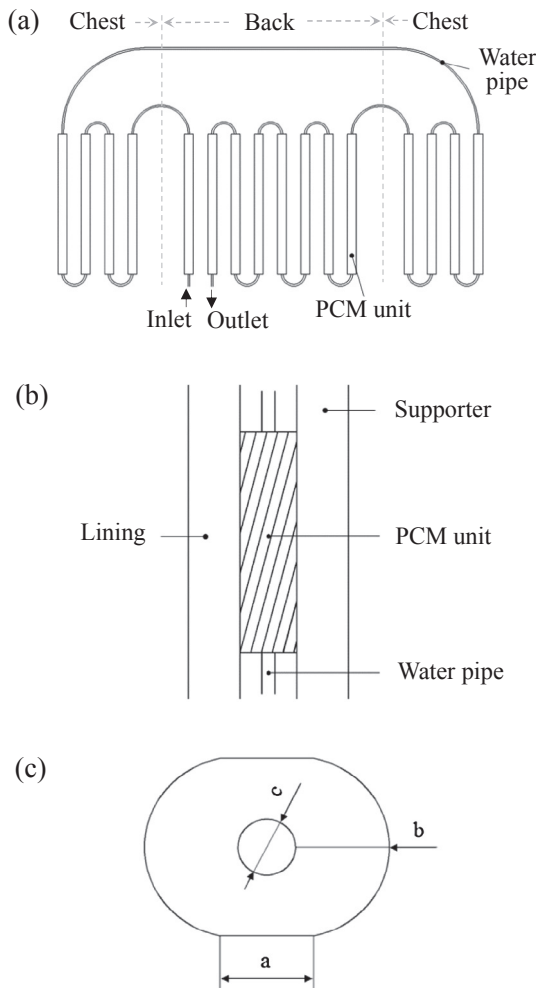


Fig. 2. Detailed structure of the PCM-liquid cooling vest (a) connection of PCM units with the pipe, (b) cross-section of PLV, (c) cross-section of a PCM unit.

PCM units, which are run through by a polyvinyl chloride (PVC) water pipe, as shown in Fig. 2(a). The PCM units are attached to a supporter and covered by a cotton lining on the side in contact with the wearer. The cross-sectional views of the cooling vest and a PCM unit are shown in Fig. 2(b) and (c). Moreover, the PLV is equipped with an insulation vest to insulate the heat transfer of the PLV with the hot environment, as required. The employed materials, sizes and physical properties of the components of the PLV are listed in Table 1. The selection of other design parameters, such as the type of PCM, flow rate and inlet temperature of the cold water under the cooling-storage mode is investigated using mathematical modeling.

3. Mathematical modeling

In the mathematical modeling, the selection of multiple design parameters and operating performance in different working conditions are investigated for the PLV under the cooling-storage mode and

Table 1
Materials, sizes and physical properties of components of the PLV.

Component	Material	Density (kg/m ³)	Specific heat (J/kg·°C)	Conductance (W/m·°C)	Geometry (mm)
Water pipe	PVC	1380	1003	0.16	3 × 5 (inner × outer diameter)
Lining	Cotton	55.6	1280	0.072	1.3 (thickness)
Support garment	Porous polyester	50	1340	0.084	2 (thickness)
Insulation Vest	Floss	28	1184	0.024	20 (thickness)

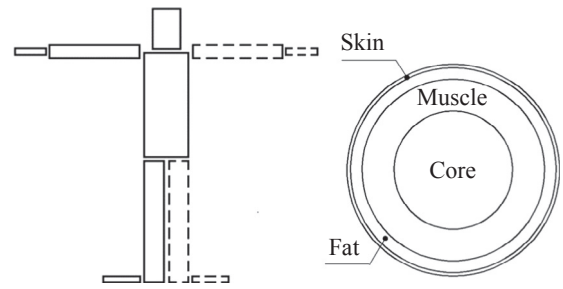


Fig. 3. Human body construction.

wearing mode. Considering the performance characteristics of the PLV—transience, regional cooling and involvement of wearer’s thermophysiological responses—a human model with thermoregulatory functions and a PLV model, which are built with the help of the finite element analysis software ANSYS, are included in the mathematical modeling.

3.1. Human model

The human body consists of several regions with distinct thermal physical and physiological characteristics. In addition, the PLV adopts regional cooling for the torso. Therefore, the body is described using Stolwijk’s 25 parts [26], as illustrated in Fig. 3. The body includes six-cylinder segments, which represent the head, arm, hand, torso, leg, and foot. Each segment consists of four tissue layers to represent the core, muscle, fat, and skin. The central blood system is described as a separate part. Based on an average man with a weight of 68 kg and a height of 176 cm, the size, thermal physical and physiological parameters are presented in Tables 2–4, according to the calculation methods used in Refs. [27–30].

In the human body, heat is produced through metabolism and transferred to the human surface by thermal conduction of the tissue, heat convection between the tissue and blood, and respiration. We ignore the respiratory heat dissipation owing to its weak effect on the total heat transfer. The heat transfer process in the human body is described using Pennes’ bioheat equation as follows [31].

$$\rho_t c_t \frac{\partial T_t}{\partial \tau} = \lambda_t \nabla^2 T_t + Q_m + Q_b \tag{1}$$

$$Q_b = B c_b (T_b - T_t) \tag{2}$$

where ρ_t is the density of the tissue, c_t and c_b are the specific heat of the tissue and blood, λ_t is the thermal conductivity of the tissue, and τ is the time.

In Pennes’ equation, the heat convection between the tissue and blood is regarded as an isotropic heat source Q_b in the tissues. Pennes assumed that the temperature of the blood perfusing into and flowing out of the tissues equals that of the central blood system T_b and the tissue temperature T_t respectively. We assume T_b to be a constant value of 37 °C. The blood perfusion rate B is determined by the thermoregulation. Considering that the exercise intensity has a significant influence on the metabolic rate Q_m , the extra heat production due to exercise is assigned to the basal metabolism of each segment’s muscular layer, as presented in Table 4, according to Ref. [30].

Table 2
Size of the body.

Segment	Radius(cm)				Length (cm)
	Skin	Fat	Muscle	Core	
Head	8.28	8.00	7.69	6.41	25.12
Trunk	13.27	13.03	11.60	7.48	64.06
Arms	4.32	4.12	3.95	2.42	52.98
Hands	1.93	1.56	1.54	1.36	19.18
Legs	5.98	5.75	5.55	3.24	74.80
Feet	2.11	1.73	1.66	1.52	21.82

Table 3
Thermal physical parameters of the body.

Tissue	Density (kg/m ³)	Specific heat (J/kg·°C)	Conductance (W/m ² ·°C)
Skin	1085	3680	0.44
Fat	920	2300	0.21
Muscle	1085	3800	0.51
Skeleton	1357	1700	0.75
Conn. Tissue	1085	3200	0.47
Blood	1059	3850	0.47

On the skin surface, heat is rejected through thermal conduction between the skin and the garment, heat convection and radiation with the environment, and evaporative heat dissipation. The evaporative heat dissipation q_e is calculated according to Eq. (3), in which the heat dissipation of sweat evaporation q_{es} is determined as per the thermoregulatory system.

$$q_e = q_{es} + 0.996(T_s - T_a) \tag{3}$$

where T_s is the temperature of the body surface, and T_a is the ambient air temperature.

The thermoregulatory functions of the human body include vasomotion, which regulates the blood perfusion rate of skin $B_{s,i}$; sweating, which regulates the heat dissipation of sweat evaporation q_{es} ; and muscle tremor, which increases the metabolic rate Q_m in the muscle tissue. Because the human body will not be in an overcooling state when a human is wearing PCGs, the muscle tremor is ignored. According to Yuan's thermoregulatory model for environments with a broad temperature range, $B_{s,i}$ and q_{es} are calculated as Eqs. (4) and (5) [30].

$$B_{s,i} = B_{s,ba,i} \frac{[1 + K_{vd,i} \max(4.8f_s + 10.8f_{co}, 0)]}{[1 + K_{vc,i} \max(-10.8f_s - 3.8f_{co}, 0)]} \tag{4}$$

$$q_{es,i} = \min[K_{es,i} \max(53.7f_s + 472f_{co}, 0) / S_{s,i}, (13.534 + 39.9v^{0.67})(t_{s,i}^- - t_a)] \tag{5}$$

where $B_{s,ba,i}$ is the basal blood perfusion rate of segment i , $K_{vd,i}$, $K_{vc,i}$, and $K_{es,i}$ are weight coefficients of skin vasodilation, skin vasoconstriction and skin surface sweating of segment i respectively, $S_{s,i}$ is the skin surface area of segment i , and v is the ambient air velocity. The

Table 4
Thermal physiological parameters of the body.

Segment	Basal Metabolic Rate (W/m ³)				Basal blood perfusion rate (kg/(s·m ³))				Distribution coefficient of exercise metabolism
	Skin	Fat	Muscle	Core	Skin	Fat	Muscle	Core	
Head	446.11	218.43	588.03	5480.27	2.2417	0.0307	0.0909	4.7471	0.00
Trunk	2165.95	59.11	475.58	3279.80	0.3012	0.0066	0.0316	5.2276	0.30
Arms	244.65	193.01	446.02	638.49	0.8014	0.0258	0.0181	0.0694	0.08
Hands	19.93	3896.66	510.54	1577.75	2.8369	0.7878	0.4679	0.3301	0.01
Legs	223.54	187.07	416.68	391.73	0.5896	0.0111	0.0163	0.0197	0.60
Feet	44.01	1171.69	529.46	1665.23	1.8390	0.1809	0.5786	0.1394	0.01
Total	86.6 W				0.0788 kg/s				-

Table 5
Set-point temperature and weighting coefficients of tissues.

Segment	Set-point temp. (°C)				Weighting coefficient			
	Skin	Fat	Muscle	Core	$K_{s,i}$	K_{vd}	K_{vc}	K_{es}
Head	35.80	36.13	36.48	37.06	0.15	0.04	0.06	0.24
Trunk	34.67	35.50	36.84	37.12	0.40	0.00	0.12	0.65
Arms	34.20	34.51	35.05	35.61	0.17	0.32	0.19	0.03
Hands	35.33	35.39	35.41	35.47	0.08	0.16	0.16	0.02
Legs	34.46	34.53	35.02	35.46	0.13	0.32	0.31	0.04
Feet	35.30	35.40	35.29	35.46	0.07	0.16	0.16	0.02

skin temperature signal f_s and the core (hypothalamus) temperature signal f_{co} are calculated as Eqs. (6)–(8).

$$f_s = \sum_{i=1}^6 K_{s,i} (t_{s,i}^- - t_{s,i, set} + R_i \frac{\partial t_{s,i}^-}{\partial \tau}) \tag{6}$$

$$R_i = \begin{cases} 0 & \frac{\partial t_{s,i}^-}{\partial \tau} > 0 \\ 10 & \frac{\partial t_{s,i}^-}{\partial \tau} < 0 \end{cases} \tag{7}$$

$$f_{co} = t_{co}^- - t_{co, set} \tag{8}$$

where $K_{s,i}$ is the weight coefficient of the skin temperature of segment i , R_i is the skin dynamic inductance, $t_{s,i, set}$ and $t_{co, set}$ are the temperature set-points of skin in segment i and hypothalamus, and $t_{s,i}^-$ and t_{co}^- are the average temperature of skin in segment i and hypothalamus. The temperature set-points $t_{s,i, set}$ and $t_{co, set}$, and weight coefficients $K_{vd,i}$, $K_{vc,i}$, $K_{es,i}$ and $K_{s,i}$ for segment i are listed in Table 5.

As described in the above equations, the skin temperatures in the segments and their changes are used to determine the thermoregulation activities. In addition, the temperature receptors and effectors of the six segments have different weights in thermoregulation. These comprehensive considerations of thermoregulatory functions of the human body can enable the performance of the PLVs to be examined in detail using mathematical modeling.

3.2. PLV model

The geometry of the PLV model is determined by the design scheme described in Section 2. For modeling the phase change process of PCM, the most popular methods are the enthalpy method and effective heat capacity method. In the PLV model, the enthalpy method is used due to its convenience, extensive usage scope, and adoption in ANSYS Fluent. The enthalpy method uses a single energy equation to describe the energy process in liquid and solid domains and at the liquid-solid interface [32]. Therefore, it is appropriate for the situation where there is no a clearly liquid-solid interface during the phase change process, and the interface does not need to be tracked. For the PCM in this PLV model, the energy equation can be expressed as Eq. (9) where the heat source and the convection are ignored. The temperature, velocity, and

mass transport equations are used to describe the heat and mass transfer process in and between other components such as pipes, water, and the lining.

$$\rho_p \frac{\partial H_p}{\partial \tau} = \lambda_p \nabla^2 T_p \tag{9}$$

where ρ_p is the density of the PCM, λ_p is the thermal conductivity of the PCM, and H_p is the enthalpy of the PCM.

3.3. Simulation performance

3.3.1. Cooling-storage mode

In the cooling-storage mode, the working performance of the PLV includes the cooling charging time and the degree of subcooling. The charging time is defined as the period from the beginning to the end of the cooling charging. The end of cooling charging is defined as the instant at which 90% of PCM in the last PCM unit in the water flow direction is frozen. The charging time reflects how fast cooling can be stored in the PLV. The degree of subcooling is defined as the temperature difference between the phase transition temperature and the PCM temperature in the first PCM unit in the water flow direction when cooling charging is complete. The degree of subcooling reflects the temperature uniformity of the PCM, which influences the comfort of PLV in the initial time of the wearing mode. With the existing design scheme, the cooling charging time and the degree of subcooling are affected by three design parameters including the type of PCM, and inlet temperature and velocity of the cold water. The influence of the type of PCM on the performance of the PLV is due to the distinct differences between density and thermal conductivity between organic and inorganic PCMs. OP27E (paraffin wax) and RE25 (inorganic salts) are considered to represent organic and inorganic PCMs, respectively. The physical parameters of OP27E and RE25, and the weight and size of the PCM units, are listed in Table 6. The phase transition temperature of OP27E is adjusted to be the same as that of RE25 to exclude the influence of phase transition temperature on the working performance of the PLV.

To simplify the PLV model in the cooling-storage mode, the following assumptions are made.

- The insulation vest can isolate the PLV with the environment in heat exchange.
- The effect of thin TPU film in heat exchange is ignored.

We formulate eight cases under the cooling-storage mode based on the three design parameters, each of which has two values. The heat transfer processes of the eight cases are simulated using the PLV model with the aid of ANSYS. The case information and simulation results are presented in Table 7.

Table 7 shows that the inorganic PCM reduces the charging time considerably owing to its high density and thermal conductivity. However, an inorganic PCM increases the degree of subcooling compared to organic PCM. The low inlet temperature of cold water reduces the charging time but increases the degree of subcooling. The higher flow rate of cold water can decrease the charging time and subcooling simultaneously. Because the three design parameters affect the charging time and the subcooling at different degrees, it is better to use inorganic PCMs in the case of a high flow rate of cold water. The inlet temperature of cold water should be determined considering the trade-

Table 6
Physical parameters of PCM and the weight and size of PCM units.

PCM	Density (kg/m ³)	Specific heat (J/kg·°C)	Conductance (W/m·°C)	Phase change latent heat (J/kg)	Phase change temp. (°C)	Mass (kg)	Size of PCM units (mm)
OP27E	760–880	2000	0.2	179,000 (180,000)	25–27 (24–26)	1.2	a × b × c = 8 × 8 × 5
RE25	1400–1500	2700	0.6	180,000	24–26	1.2	a × b × c = 6 × 6 × 5

Table 7
Case information and simulation results in the cooling-storage mode.

Case no.	PCM	Inlet temp. of cold water (°C)		Velocity of cold water (m/s)		Charging time (min)	Degree of subcooling (°C)
		10	5	0.5	1.5		
C1	√	√		√		72	5.8
C2	√	√			√	66	3.7
C3	√		√	√		56	11
C4	√		√		√	55	5
C5		√	√		√	51	10.8
C6	√	√			√	41	5.6
C7	√		√	√		38	15
C8	√		√		√	35	10

off between the charging time and subcooling. As shown in Fig. 2(a), a water pipe runs along the 16 PCM units serially, which is the main reason for the subcooling of PCM. To reduce the degree of subcooling, an improvement measure could be the use of multiple parallel water pipes. Taking case 6 as an example, the degree of subcooling and charging time are reduced to 3.9 °C and 33 min, respectively, when we consider four parallel pipes in the PLV and each pipe runs through 4 PCM units serially.

3.3.2. Wearing mode

In the wearing mode, the working performance of the PLV (with RE25) includes the service time and cooling rate of the PLV, and the skin temperature of the human body. The service time refers to the period from the beginning of wearing to the end when PCM has melted completely. The cooling rate of the PLV refers to the heat transfer rate from the environment and the human body to the PCM. In the wearing mode, the situation in which the PLV is applied in an indoor office in summer is considered. The influence of indoor temperature, vest tightness and the insulation vest on the performance of the PLV is investigated. The vest tightness is represented by different shapes of the cross-section of the PCM units, as illustrated in Table 8. The metabolism rate of the average person working at the office is 116.35 W.

To simplify the model in the wearing mode, the following assumptions are made:

- The water pipe is ignored owing to the lack of circulated water for cooling-storage.
- The TPU film is ignored owing to its thinness.
- The PLV is in direct contact with the body.
- Moisture transfer and perspiration condensation are ignored.
- Radiation heat transfer of the outside surfaces of the wearer and vest with the environment is ignored.
- PCM flow due to gravity and density difference during the melting process are ignored.
- Convection heat transfer coefficient is 3.34 W/m²·°C.

We formulate eight cases in the wearing mode based on the three influential factors, each of which has two values. The details of the eight cases are presented in Table 9. The heat transfer processes of the eight cases are simulated using the human model and PCG model with the aid of ANSYS. The initial temperature of the human body set in the human model is derived from the simulation of the human body being

Table 8
Shapes of the cross-section of PCM units.

Tightness	Dimension of PCM units (mm)
Loose	$a \times b \times c = 6 \times 6 \times 5$
Tight	$a \times b \times c = 16.9 \times 4 \times 5$

steady in the indoor environment without the use of PLV. The simulation results are shown in Table 9, which presents the temperature variation rate of the skin covered by the PCM units in the initial stage (T') and the average temperature of that part of the skin in steady stage (T) for each case. The initial stage refers to the period of five minutes after the wearer puts on the PLV. The steady stage refers to the period when the temperature of the skin covered by the PCM units keeps relatively steady. For case 1, the temperature variation profiles for seven regions of the human body is shown in Fig. 4, and the temperature distribution of the human body and a PCM unit in 40 min are shown in Fig. 5. The skin temperature for the other seven cases has the same tendency of variation as in case 1.

As shown in Fig. 4, the skin temperature of the cooled part on the trunk reduces rapidly after the wearer puts on the PLV and then remains stable for a large duration. At the end of the service time (225 min), the skin temperature of the cooled part on the trunk is lower than the initial value ($35.7 \text{ }^\circ\text{C}$) because the completely melted PCM still has the cooling capacity at this time. For all other regions of the human body, the skin temperature reduces slightly when the PLV is used. This phenomenon is caused by the vasoconstriction in the skin all over the body after the thermoregulatory center receives the cold signal from the cooled trunk.

For the three influential factors, the simulation results of the eight cases (shown in Table 9) indicate that vest tightness exerts the maximum influence on the cooling performance of the PLV compared to the other two factors. The vest tightness affects the heat transfer between the PLV and the body by changing the contact area. The indoor air temperature and insulation vest affect the heat transfer between the PLV and the environment. Therefore, the heat conductivity between the PLV and the human body is the main medium for cool discharge of the PCM. Studies show that the temperature of the human body determines the thermal sensation and comfort [33]. The considerable influence of the vest tightness on the skin temperature inspires wearers to adjust the tightness of the vest to increase comfort. In addition, adjustment of the vest tightness can enable the PLV to be useful under different environment temperatures and exercise scenarios. The use of the insulation vest and the ambient air temperature affect the service time and cooling rate of the PLV but they have minimal effect on the human body. Thus, the insulation vest can be used to prolong the service time of the PLV, especially when there is a large cool discharge to the environment due to the large air velocity or heat radiation.

Table 9
Case information and simulation results in the wearing mode.

Case no.	Indoor temp. ($^\circ\text{C}$)		Vest tightness		Insulation vest		Service time (min)	Cooling rate (W)	T' ($^\circ\text{C}$)	T ($^\circ\text{C}$)
	30	34	loose	tight	without	with				
C1	✓		✓		✓		225	15.3	4.5	32.7
C2	✓		✓			✓	257	13.4	4.7	32.7
C3	✓			✓	✓		178	19.4	6.6	31.3
C4	✓			✓		✓	206	16.7	7.0	31.3
C5		✓	✓		✓		207	16.7	4.6	32.9
C6		✓	✓			✓	239	14.4	4.6	32.9
C7		✓		✓	✓		171	20.2	6.8	31.6
C8		✓		✓		✓	186	18.5	7.0	31.5

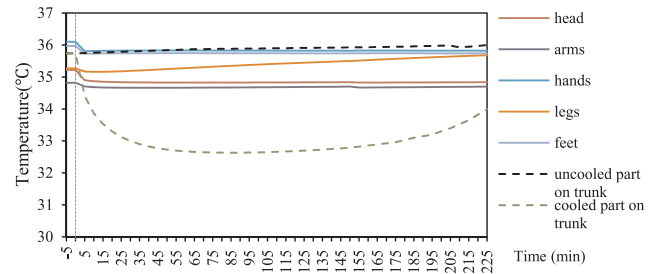


Fig. 4. Temperature change profiles for the human body.

4. Human trial

A set of cooling-storage trials and wearing trials were conducted in a climate chamber. The temperature, humidity and fresh air rate of the climate chamber were controlled at $30 \text{ }^\circ\text{C}$, 45% and $20 \text{ m}^3/\text{h}$, respectively. The PLV for the human trial contained 1.2 kg of RE25 and had a total mass of 1.8 kg. The PLV and experimental scenarios are shown in Fig. 6.

4.1. Cooling-storage trial

The cooling-storage trial is shown in Fig. 6(b). The PLV is connected with a microchiller and charged by the cold water from the chiller. The inlet temperature of the cold water is $5 \text{ }^\circ\text{C}$ and the velocity is 0.5 m/s . During the cooling-storage period, the PLV is enveloped with the insulation vest to isolate the ambient hot air. The temperature of the PCM units at four points is measured and recorded by thermometers. The cooling-storage experiment is consistent with case 7 in Table 7. Fig. 7 shows the measured temperature variation of the PCM and its agreement with the simulation results. The model results match with the experiment data in general, and there is a deviation of the values obtained from the simulation results in the initial and end stages. In the cooling-storage trial, the temperature of the PCM first reduces from the ambient air temperature, then remains at the phase transition temperature, and reduces again after subcooling of a part of the PCM. In the initial and end stages, the part of the PCM is not in the phase transition process. The reason of the deviation in the initial and end stages might be that the measured result at four points cannot well represent the overall temperature of the PCM as obtained from the simulation when part of the PCM is not in the phase transition process.

4.2. Wearing trial

The wearing trial is shown in Fig. 6(c). Eight healthy male volunteers participated in the experiment. The average age, height, and weight of the eight volunteers were 24, 176.9 cm, and 71.1 kg, respectively. Before wearing the cooling vest, the volunteers wore short-sleeved shirts, shorts, and sandals, and read books in the climate chamber for approximately 1 h. This process aimed to make volunteers

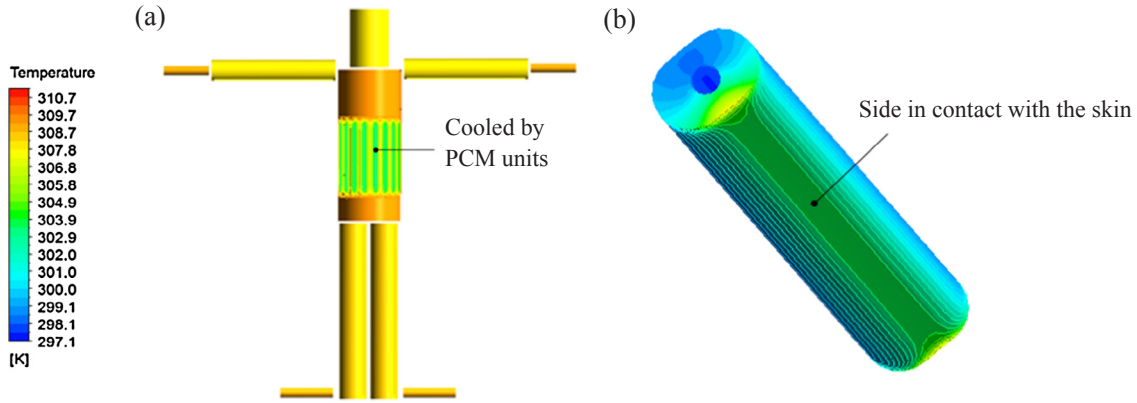


Fig. 5. Temperature distribution. (a) Human body (b) PCM unit.

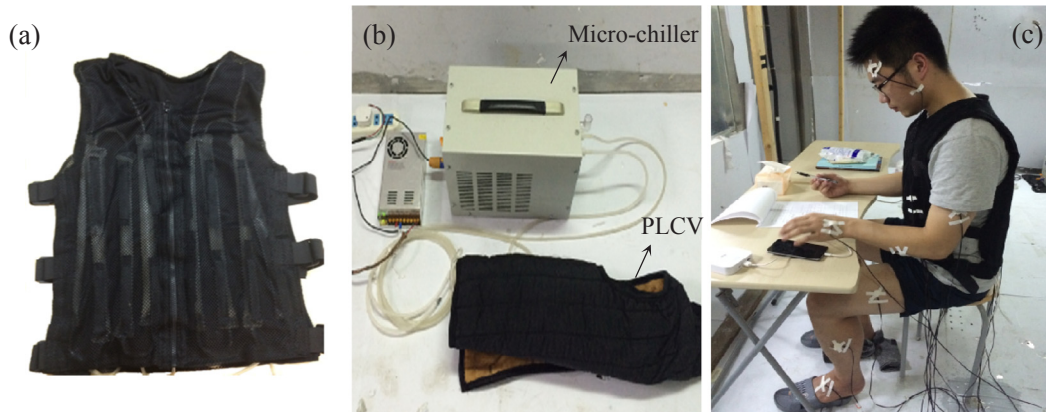


Fig. 6. PLV and experimental scenarios. (a) PLV, (b) cooling-storage trial, (c) wearing trial.

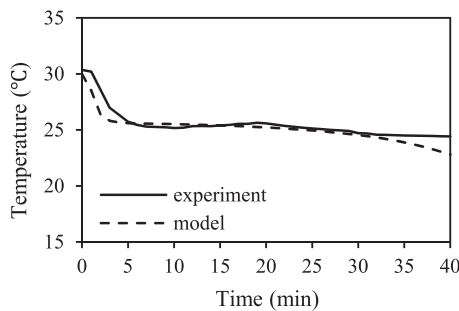


Fig. 7. Comparison of simulation results with measured data for PCM freezing.

adapt to the hot environment. After the volunteer’s body reached the thermal steady state, the volunteers put on the cooling vest and the two-hour wearing experiment commenced. The temperature of the skin at 11 points on the wearers (as Fig. 8) was measured and recorded by thermometers in real time from 5 min before to the end of the wearing experiment. During this time, volunteers recorded, in questionnaires, in intervals, the local thermal sensation and comfort of the skin covered by the PCM units and the overall thermal sensation and comfort. The thermal sensation scale and comfort scale in the experiment are shown in Fig. 9 [34–36]. The temperature of the PCM units at the four points was measured and recorded using thermometers. The wearing experiment was consistent with case 1 presented in Table 9.

The comparison of the measured data with the simulation results is shown in Figs. 10 and 11, which describe the temperature variation of the body parts and PCM with time in the wearing mode. According to Fig. 10, the simulated local temperatures for the trunk and arms agree well with the experimental data, and the deviation is within 0.5 Å°C

and 0.3 Å°C. Compared with the trunk and arms, the simulated local temperatures for the head, hands, legs and feet have a slightly larger deviation from experimental data although the simulated and experimental temperature exhibit the same variation trend. For the head, hands, legs and feet, the deviation is within 1.1, 1.3, 1.7 and 1.4 Å°C, respectively. These deviations for the skin temperature are mainly caused by the errors in the human model and insufficient measurement points for the skin temperature in the experiment. For example, the

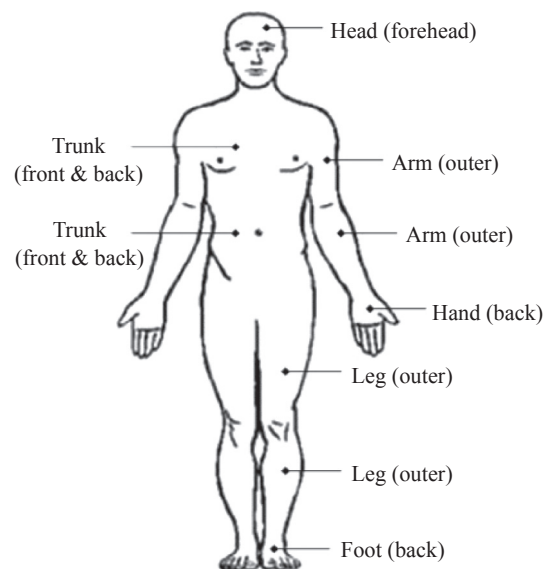


Fig. 8. Skin temperature measurement locations.

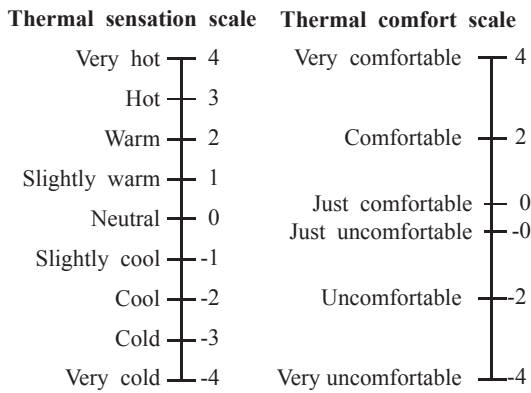


Fig. 9. Thermal sensation and comfort scale.

forehead temperature measured at one point in the experiment cannot well represent the overall head skin temperature in the simulation. For the PLV, the simulation results of the melting process of the PCM coincide with the experimental data except for those at the end of cooling-discharge, with a maximum error of 1.5 °C, as shown in Fig. 11. In the wearing experiment, the PCM will flow in the PCM units when melting owing to gravity and the difference in density between the liquid and solid phases. The temperature at the four measurement points cannot well represent the overall PCM temperature when the solid and liquid PCM stratifies vertically. In addition, for simplification of the PLV model, the stratification is not considered in the simulation. Therefore, the stratification phenomenon in the experiment and simplification of the PLV model are the main reasons for the deviation between the simulated and experimental results for the PCM temperature.

The local thermal sensation (L-S) and local thermal comfort (L-C) of the skin covered by the PCM units, and the overall thermal sensation (O-S) and overall thermal comfort (O-C) of the complete body during the wearing process is presented in Fig. 12. After the volunteers put on the cooling vest, the local and overall thermal sensation reduces rapidly. The value of the local comfort reduces gradually owing to the sudden cool sensation on the trunk but the overall comfort increases at the same time. During the two hours of the wearing process, the local

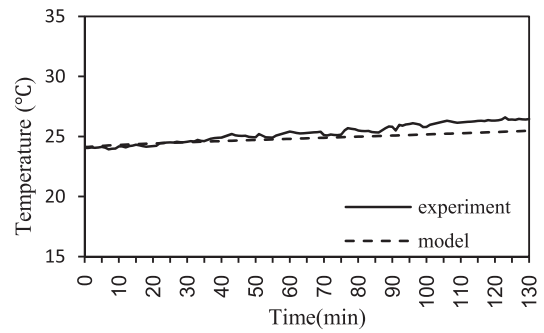


Fig. 11. Comparison of simulation results with measured data for PCM melting.

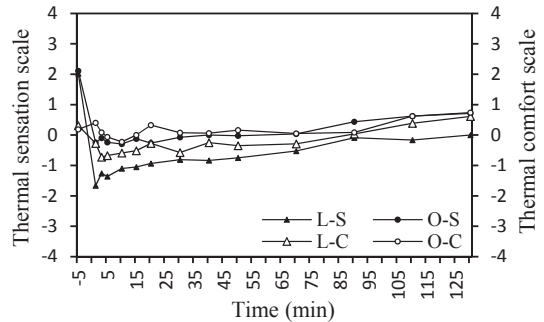


Fig. 12. Local and overall thermal sensation and comfort recorded in the human trial.

sensation, overall sensation, local comfort and overall comfort remain close to the corresponding levels of slightly cool, neutral, just uncomfortable and just comfortable, respectively. The comparison of the overall sensation and comfort before and after the use of the PLV indicates that the regional cooling vest can help maintain the heat balance of the entire body without sacrificing the overall thermal comfort although there is a little uneven thermal sensation.

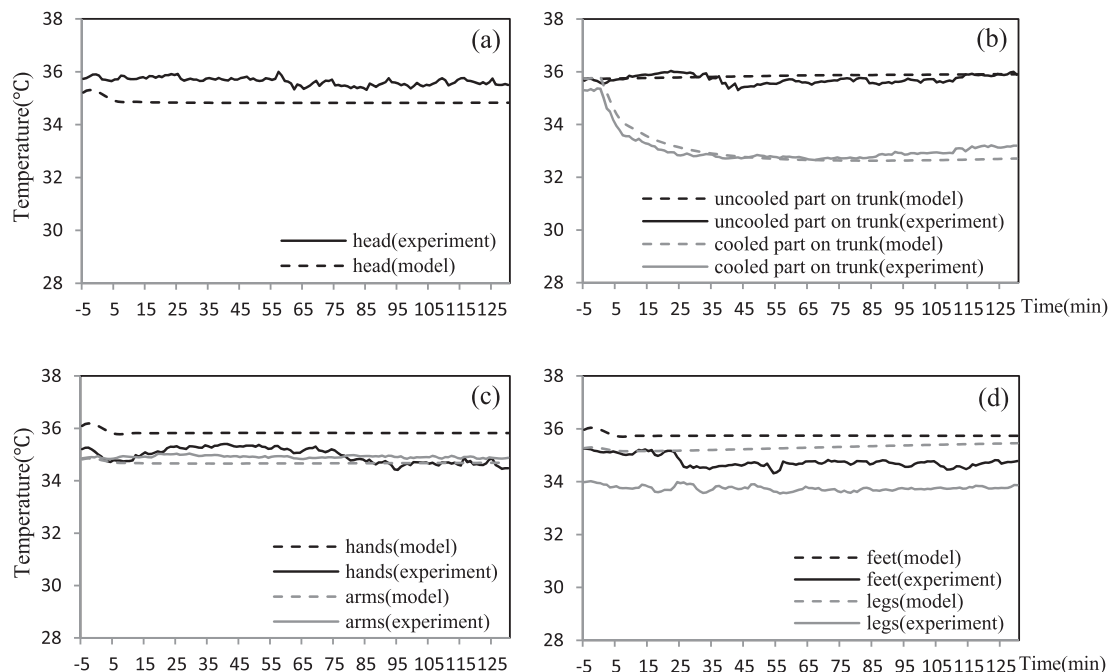


Fig. 10. Comparison of simulation results with measured data for the human body.

5. Conclusion

This paper proposes a new type of PCG, the PCM-liquid cooling vest, to enhance the convenience of cooling-storage for PCM garments. The scheme of the PLV combines PCM with water pipes buried in the PCM. The PCM in the vest is used to cool the torso and the water pipe buried in the PCM is used to circulate cold water from a microchiller to freeze the PCM. This method of cooling charge enables PLV storage cooling at any given time without interrupting the use of PLV for wearers.

To determine some design parameters and analyze the performance of PLV under different working conditions, mathematical modeling and a human trial are conducted. Based on the simulation results, the use of inorganic PCM with high density and conductivity, a high flow rate of cold water, and multiple parallel water pipes buried in PCM are recommended to reduce the charging time and the degree of subcooling in the cooling-storage mode. In the wearing mode, adjusting the tightness of the vest by the wearer is an effective way to make the PLV more comfortable and adaptable to different environments and exercise scenarios. The insulation vest can effectively isolate the heat transfer between the PLV and the environment and thus prolong the service time.

The validation of the mathematical modeling and evaluation of the PLV in terms of the thermal sensation and comfort are conducted through the human trial. The experimental verification indicates that the mathematical modeling can accurately simulate the heat transfer between the PCGs and the wearer and predict the working performance of the PLV. The simulated temperature of the PCM in the PLV coincides with the experimental data except for at the start or end in the cooling-storage or wearing mode with a maximum error $1.6\text{ }^{\circ}\text{C}$. For the trunk, which is the part of the human body involved in the heat transfer process with the PLV, the deviation of simulated temperature from the experimental data is within $0.5\text{ }^{\circ}\text{C}$. For other parts of the human body, the deviation is within $0.3\text{ }^{\circ}\text{C}$, $1.1\text{ }^{\circ}\text{C}$, $1.3\text{ }^{\circ}\text{C}$, $1.7\text{ }^{\circ}\text{C}$ and $1.4\text{ }^{\circ}\text{C}$, respectively. The small deviation for the trunk and the PCM during the phase transition process indicates that the mathematical modeling can accurately simulate the heat transfer between PCGs and the wearer and predict the working performance of the PLV. According to the filled questionnaires, the local sensation, overall sensation, local comfort and overall comfort remain at the corresponding levels of slightly cool, neutral, just uncomfortable and just comfortable, respectively. The local and overall thermal sensation votes indicate that the regional cooling vest can help maintain the heat balance of the entire body without sacrificing the overall thermal comfort. The selection of the PCM with a slightly higher phase transition temperature than that of RE25 may be a measure to increase the local comfort of the cooled region. But for the regional cooling, it is hard to have both the neutral and comfort of the cooled region and the whole body.

According to the human trial, the PLV with a total mass of 1.8 kg can provide the wearer with effective cooling for at least 2 h , which can allow the wearer to walk for 7.2 km if the walking speed is approximately 1 m/s . When the cooling-storage and wearing combined mode is required, the large difference between the charging time (40 min) in the cooling-storage mode and the service time (at least 2 h) in the wearing mode can guarantee effective cooling-storage within 60 min . Owing to the characteristics of temperature stability around the phase transition temperature, the person wearing a PLV will experience the same thermal sensation and comfort in the cooling-storage and wearing combined mode as in the single wearing mode.

Acknowledgements

This work was supported by National Science & Technology Pillar Program during the thirteenth Five-year Plan Period (2017YFB0903404).

References

- [1] N.A.S. Taylor, Challenges to temperature regulation when working in hot environments, *Ind. Health* 44 (2006) 331–344.
- [2] G.B. Delkumburewatte, T. Dias, Wearable cooling system to manage heat in protective clothing, *J. Text. Inst.* 103 (2012) 483–489.
- [3] F.E. Marino, Methods, advantages, and limitations of body cooling for exercise performance, *Brit. J. Sports Med.* 36 (2002) 89–94.
- [4] M.J. Barwood, S. Davey, J.R. House, M.J. Tipton, Post-exercise cooling techniques in hot, humid conditions, *Euro. J. Appl. Physiol.* 107 (2009) 385–396.
- [5] J.H. Kim, A. Coca, W.J. Williams, R.J. Roberge, Effects of liquid cooling garments on recovery and performance time in individuals performing strenuous work wearing a firefighter ensemble, *J. Occup. Environ. Hygiene* 8 (2011) 409–416.
- [6] M.M. Yazdi, M. Sheikhzadeh, Personal cooling garments: a review, *J. Text. Inst.* 105 (2014) 1231–1250.
- [7] M.M. Zhao, C.S. Gao, F.M. Wang, K. Kuklane, I. Holmer, J. Li, A study on local cooling of garments with ventilation fans and openings placed at different torso sites, *Int. J. Ind. Ergon.* 43 (2013) 232–237.
- [8] VESKIMO. < <http://www.veskimo.com/> > .
- [9] D.P. Colvin, Y.G. Bryant, Micro-Climate Cooling Garment, US5415222A, Delta Thermal Systems Inc, U.S., 1995.
- [10] B.A. Ying, Y.L. Kwok, Y. Li, Q.Y. Zhu, C.Y. Yeung, Assessing the performance of textiles incorporating phase change materials, *Polym. Test.* 23 (2004) 541–549.
- [11] M.M. Yazdi, M. Sheikhzadeh, S. Borhani, Modeling the heat transfer in a PCM cooling vest, *J. Text. Inst.* 106 (2015) 1003–1012.
- [12] D.Y. Lee, Y.S. Hwang, Subminiature cool pad applying sorption cooling effect, *Hvach & Res.* 12 (2006) 797–806.
- [13] M. Rothmaier, M. Weder, A. Meyer-Heim, J. Kesselring, Design and performance of personal cooling garments based on three-layer laminates, *Med. Biol. Eng. Comput.* 46 (2008) 825–832.
- [14] Y.F. Yang, J. Stapleton, B.T. Diagne, G.P. Kenny, C.Q. Lan, Man-portable personal cooling garment based on vacuum desiccant cooling, *Appl. Therm. Eng.* 47 (2012) 18–24.
- [15] T.C. Ernst, S. Garimella, Demonstration of a wearable cooling system for elevated ambient temperature duty personnel, *Appl. Therm. Eng.* 60 (2013) 316–324.
- [16] N.A. Pimental, H.M. Cosimini, M.N. Sawka, C.B. Wenger, Effectiveness of an air-cooled vest using selected air-temperature and humidity combinations, *Aviat. Space Environ. Med.* 58 (1987) 119–124.
- [17] S. Mondal, Phase change materials for smart textiles – an overview, *Appl. Therm. Eng.* 28 (2008) 1536–1550.
- [18] N. Bogerd, A. Psikuta, H.A.M. Daanen, R.M. Rossi, How to measure thermal effects of personal cooling systems: human, thermal manikin and human simulator study, *Physiol. Meas.* 31 (2010) 1161–1168.
- [19] Z.X. Guan Ping, Li Jun, Zhu Yingxin, Experimental study on thermal comfort of medical phase change cooling garment, Proceedings of the National Academic Conference on Heating, Ventilating, Air Conditioning and Refrigeration in 2004, 2004, pp. 323–328.
- [20] J.A. Gonzalez, L.G. Berglund, M.A. Kolka, T.L. Endrusick, Forced ventilation of protective garments for hot industries, *Therm. Manik. Model.* (2006) 165.
- [21] L.-N. Li, X.-M. Qian, J.-T. Fan, Test and analysis of cooling performance of cooling garments, *J. Tianjin Polytech. Univ.* 5 (2008) 015.
- [22] A. Psikuta, M. Richards, D. Fiala, Single-sector thermophysiological human simulator, *Physiol. Meas.* 29 (2008) 181.
- [23] Y.F. Qiu, N. Jiang, W. Wu, G.W. Zhang, B.L. Xiao, Heat transfer of heat sinking vest with phase-change material, *Chin. J. Aeronaut.* 24 (2011) 720–725.
- [24] S. Ghani, E.M.A.A. ElBialy, F. Bakochristou, S.M.A. Gamaledin, M.M. Rashwan, The effect of forced convection and PCM on helmets' thermal performance in hot and arid environments, *Appl. Therm. Eng.* 111 (2017) 624–637.
- [25] F.L. Tan, S.C. Fok, Cooling of helmet with phase change material, *Appl. Therm. Eng.* 26 (2006) 2067–2072.
- [26] J.A. Stolwijk, A Mathematical Model of Physiological Temperature Regulation in Man, 1971.
- [27] H. Arkin, A Model of Thermoregulation in the Human Body, 84-WA/HT-66, 1984.
- [28] Z. Lou, W.-J. Yang, Whole body heat balance during the human thoracic hyperthermia, *Med. Biol. Eng. Comput.* 28 (1990) 171–181.
- [29] J. Werner, M. Buse, Temperature profiles with respect to inhomogeneity and geometry of the human body, *J. Appl. Physiol.* 65 (1988) 1110–1118.
- [30] X. Yuan, Mathematical Simulation of the Human Thermal Regulation System, Chapter 5, University of Aeronautics and Astronautics Press, Beijing, 2005.
- [31] H.H. Pennes, Analysis of tissue and arterial blood temperatures in the resting human forearm, *J. Appl. Physiol.* 1 (1948) 93–122.
- [32] M. Zukowski, Mathematical modeling and numerical simulation of a short term thermal energy storage system using phase change material for heating applications, *Energy Convers. Manage.* 48 (2007) 155–165.
- [33] C. Huizenga, Z. Hui, E. Arens, A model of human physiology and comfort for assessing complex thermal environments, *Build. Environ.* 36 (2001) 691–699.
- [34] H. Zhang, E. Arens, C. Huizenga, T. Han, Thermal sensation and comfort models for non-uniform and transient environments, Part III: Whole-body sensation and comfort, *Build. Environ.* 45 (2010) 399–410.
- [35] H. Zhang, E. Arens, C. Huizenga, T. Han, Thermal sensation and comfort models for non-uniform and transient environments: Part I: Local sensation of individual body parts, *Build. Environ.* 45 (2010) 380–388.
- [36] H. Zhang, E. Arens, C. Huizenga, T. Han, Thermal sensation and comfort models for non-uniform and transient environments, Part II: Local comfort of individual body parts, *Build. Environ.* 45 (2010) 389–398.